

Quantum Circuit for Non-Unitary Linear Transformation of Basis Sets

Guorui Zhu

School of Mathematical Sciences, Fudan University

Joel Bierman

Electrical and Computer Engineering, North Carolina State University

Jianfeng Lu

*Department of Mathematics, Department of Physics and Department of Chemistry, Duke University**

Yingzhou Li

School of Mathematical Sciences, Shanghai Key Laboratory for Contemporary Applied Mathematics, Fudan University and Key Laboratory of Computational Physical Sciences, Ministry of Education†

This paper introduces a novel approach to implementing non-unitary linear transformations of basis on quantum computational platforms, a significant leap beyond the conventional unitary methods. By integrating Singular Value Decomposition (SVD) into the process, the method achieves an operational depth of $O(n)$ with about n ancilla qubits, enhancing the computational capabilities for analyzing fermionic systems. The non-unitarity of the transformation allows us to transform a wave function from one basis to another, which can span different spaces. By this trick, we can calculate the overlap of two wavefunctions that live in different (but non-distinct Hilbert subspaces) with different basis representations. This provides the opportunity to use state specific ansatzes to calculate different energy eigenstates under orbital-optimized settings and may improve the accuracy when computing the energies of multiple eigenstates simultaneously in VQE or other framework. It allows for a deeper exploration of complex quantum states and phenomena, expanding the practical applications of quantum computing in physics and chemistry.

I. INTRODUCTION

Solving many-body Schrödinger equation is one of the most promising applications on quantum computers, especially in the era of noisy intermediate-scale and early fault-tolerant quantum computing. Quantum algorithms that could be applied to solve the many-body Schrödinger equation include but not limited to variational quantum algorithms (VQAs) [1–4], quantum phase estimation (QPE) [5–8], quantum simulation [9], etc. On digital quantum computers, the many-body Schrödinger equation first needs to be discretized on a basis set, and then the discretized operator and wavefunction need to be represented by quantum circuits and a quantum state, respectively. Throughout the computation, when a change of basis set is performed, i.e., a linear transformation of the basis set, we could either recalculate coefficients on classical computer and restart the quantum algorithm, or carry out the linear transformation via a quantum circuit. Implementing quantum circuit for the linear transformation is mandatory under various scenarios, e.g., calculating the inner product between two many-body wavefunctions discretized by different basis sets. When two basis sets are unitary linear transformations of each other, the corresponding linear transformation is unitary and the quantum circuit has been studied in [10–12]. When two

basis sets are not unitary linear transformations of each other, the corresponding linear transformation is non-unitary, for which the quantum circuit implementation is proposed by this paper.

Unitary linear transformation of basis set plays an important role in quantum physics and chemistry. Hartree-Fock method [13–19] looks for the optimal unitary linear transformation of basis set such that the single Slater determinant minimizes the energy of the many-body Hamiltonian operator. Unitary linear transformations of basis set are also used widely in basis set optimization methods, e.g., natural orbital rotation [15–19], complete active space self-consistent field method (CASSCF) [20–34], optimal orbital full configuration interaction (OptOrbFCI) [35], etc. Such unitary linear transformations of basis sets are combined with quantum algorithms for ground state calculation [36–39] to boost the power of quantum computer and pursuing the infinite basis set limit. The unitary linear basis transformation can also be adopted in quantum algorithms for excited states calculation [37, 38, 40] as long as they use the same basis set to represent both ground state and low-lying excited states of the system.

Several prior works studied the quantum circuit implementation of the unitary linear transformation of basis set. The unitary coupled cluster (UCC) method [41–45], particularly with single excitation operators, is widely used as parameterized ansatz circuits for wavefunctions. UCC is achieved by employing an operator $e^{\hat{T}}$, where \hat{T} is anti-Hermitian and represented as $\sum_{i<j} t_{ij}(\mathbf{a}_i^\dagger \mathbf{a}_j - \mathbf{a}_j^\dagger \mathbf{a}_i)$. Trotter splitting is then adopted to approximate the op-

* Corresponding author: jianfeng@math.duke.edu

† Corresponding author: yingzhouli@fudan.edu.cn

erator by a quantum circuit [46–49]. While this UCC quantum circuit is not designed for unitary basis transformation, it could be used as a unitary transformation of the basis set, which is mathematically guaranteed by Thouless theorem [50]. Some other methods are proposed when they consider preparing the Slater determinant state by rotating the basis set. Wecker *et al.* [10] describe a procedure in which they use a quantum circuit to take unitary transformation of a basis set and prepare arbitrary Slater determinant state. Their circuit has no more than n^2 gates with arbitrary connectivity for n being the size of the basis set. Babbush *et al.* [12] suggest employing the fermionic fast Fourier transform to prepare a Slater determinant state in a plane wave basis. This approach involves rotating the system from a plane wave dual basis, achieving a depth of $O(n)$ while adhering to the planar lattice connectivity constraints found in some existing superconducting quantum platforms [12]. The plane wave dual basis serves as a smooth approximation to a grid structure, which has been explored to enhance the efficiency of density functional calculations [51, 52]. In [11], an efficient strategy is proposed to conduct the unitary linear transformation on a quantum computer with linearly connected qubits, and achieves a gate depth $\frac{n}{2}$, where the gate depth is counted as the number of sequential Givens rotations. The strategy is a variant of the QR decomposition based method of constructing single-particle unitary transformations [10, 53, 54]. Kivlichan *et al.* [11] organize the Givens rotations in QR decomposition in a particular ordering to benefit from the parallelization on linearly connected quantum computer and eliminates redundant rotations based on the symmetry of the Hamiltonian. Some of these unitary linear transformation methods [11, 12] target the quantum circuit implementations of initial state preparations.

Non-unitary linear transformations of basis sets also play an important role in quantum physics and chemistry for both ground state and excited state computations. In ground state computations, for example, Jiménez-Hoyos *et al.* [55] use the non-unitary Thouless theorem [50] to rotate a orthogonal basis Hartree-Fock state to a non-orthogonal basis Hartree-Fock state. Jiménez-Hoyos *et al.* [55] derive the formulas of the Hamiltonian matrix elements of this non-orthogonal Hartree-Fock state. In the excited state computation, if different basis sets (either different basis sets or different transformations of a basis set) are adopted for the ground state and low-lying excited states, calculating the overlap between different states involves a non-unitary linear transformation of basis set. Such a state-specific rotation method for excited state computation could be viewed as a multi-reference (MR) method [56, 57]. Several studies have shown that the integration of state-specific methods with CASSCF can yield higher accuracy, even with a reduced active space [58–61]. Such an approach is referred to as the state-specific CASSCF (SS-CASSCF). SS-CASSCF employs different reference states to generate configuration interaction (CI) functions and incorporates an ap-

propriate orthogonal penalty into the objective function. The computation of this orthogonal penalty requires computing the inner product between two states under different bases. In general, if the states exhibit dense configurations, the calculation of such inner products scales exponentially with respect to the basis set size on classical computers. Computing such inner products under special cases, *e.g.* Hartree-Fock state or sparse states, has been explored on classical computers [56, 57, 62–66].

In this work, we propose a quantum circuit that performs the exact non-unitary linear transformation of a basis set. The gate complexity of the proposed quantum circuit scales polynomially in the basis set size, more specifically scales quadratically in the basis set size, *i.e.*, $O(n^2)$ for n being the basis set size. The circuit depth scales linearly in the basis set size. Combined with regular inner product quantum circuit, we could evaluate the inner product of two states under different basis sets with $O(n^2)$ gates and $O(n)$ depth on a quantum computer. Our major contributions are summarized as follows.

1. We rewrite the unitary linear transformation of basis set using wedge exterior notation, which can then be easily extended to the non-unitary case.
2. A quantum circuit is proposed for non-unitary linear transformations of basis sets. The 1 and 0 singular values of the overlapping matrix between two basis sets are further compressed to reduce the gate complexity.
3. Quantum circuits are proposed to evaluate the inner product of two states in different basis sets.

The rest of the paper is organized as follows. In Section II, we review the quantum circuit for unitary linear transformations [11] and rewrite the derivation of the unitary transformation operator in the language of exterior algebra. Section III proposes the novel quantum circuit for performing non-unitary linear transformations of basis set. The corresponding gate complexity and circuit depths are analyzed as well. Based on the non-unitary linear transformation, quantum circuits with depth $O(n)$ are proposed for evaluating the inner product of two states under different basis sets in Section IV. Finally, Section V concludes the paper together with discussions on future work.

II. UNITARY LINEAR TRANSFORMATION

We review the quantum circuit for unitary linear transformation proposed by Kivlichan *et al.* [11] and rewrite the derivation using exterior algebra in this section.

The unitary linear transformation of basis set discussed in [11] admits,

$$|\phi_p\rangle = \sum_{q=1}^n |\psi_q\rangle u_{qp} \quad (1)$$

where u is an $n \times n$ unitary matrix, $\{|\psi_i\rangle\}_{i=1}^n$ and $\{|\phi_i\rangle\}_{i=1}^n$ are the original and rotated orthonormal basis (spin-orbitals) respectively, and n denotes the basis set size. The associated creation and annihilation operators admit a similar transformation relationship,

$$\mathbf{a}^\dagger(\phi_p) = \sum_{q=1}^n \mathbf{a}^\dagger(\psi_q) u_{qp} \quad \text{and} \quad \mathbf{a}(\phi_p) = \sum_{q=1}^n \mathbf{a}(\psi_q) (u_{qp})^*,$$

where $\mathbf{a}^\dagger(\cdot)$ and $\mathbf{a}(\cdot)$ are the creation and annihilation operators associated with the given basis, and $(u_{qp})^*$ is the complex conjugate of u_{qp} .

Given the two one-body basis sets, $\{|\psi_i\rangle\}_{i=1}^n$ and $\{|\phi_i\rangle\}_{i=1}^n$, we could generate two many-body basis sets to represent the many-body states. For two one-body basis sets that are related to each other by a unitary linear transformation, as in (1), their associated many-body basis sets are also related to each other by a unitary linear transformation. The unitary linear transformation in many-body space is characterized by the Thouless theorem [50], which is equivalent to applying the operator,

$$U(u; \psi) = \exp\left(\sum_{p,q=1}^n (\log u)_{pq} \mathbf{a}^\dagger(\psi_p) \mathbf{a}(\psi_q)\right) \quad (2)$$

to the many-body states, where $(\log u)_{pq}$ denotes the (p, q) element of the matrix $\log u$. The notation ψ in $U(u; \psi)$ denotes that all creation and annihilation operators correspond to the basis set $\{|\psi_i\rangle\}_{i=1}^n$.

Now we give a definition of this $U(u; \psi)$ in the language of exterior algebra. Given an n dimensional Hilbert space V with $\{|\psi_i\rangle\}_{i=1}^n$ being its orthonormal basis set, the k -th exterior powers is denoted as $\wedge^k V$. A basis set of $\wedge^k V$ admits,

$$\{|\psi_{i_1}\rangle \wedge \cdots \wedge |\psi_{i_k}\rangle \mid 1 \leq i_1 < \cdots < i_k \leq n\}. \quad (3)$$

The bases in (3) are orthonormal. For the electronic many-body Schrödinger equation, the k -particle states live in $\wedge^k V$. The exterior algebra of V is defined as, $\wedge V = \bigoplus_{k \geq 0} \wedge^k V$. An orthonormal basis set of $\wedge V$ admits,

$$\{|\psi_{i_1}\rangle \wedge \cdots \wedge |\psi_{i_k}\rangle \mid 1 \leq i_1 < \cdots < i_k \leq n \text{ and } k \geq 0\}. \quad (4)$$

The space $\wedge V$ is also known as the Fock space in physics and chemistry. In the following Definition 1, we extend a linear map $\mathbf{u} : V \rightarrow V$ to a linear map $\wedge \mathbf{u} : \wedge V \rightarrow \wedge V$.

Definition 1. Let $\mathbf{u} : V \rightarrow V$ be a linear map. Define $\wedge \mathbf{u} : \wedge V \rightarrow \wedge V$ as,

$$\wedge \mathbf{u}(|\psi_{i_1}\rangle \wedge |\psi_{i_2}\rangle \wedge \cdots \wedge |\psi_{i_k}\rangle) = \mathbf{u}|\psi_{i_1}\rangle \wedge \mathbf{u}|\psi_{i_2}\rangle \wedge \cdots \wedge \mathbf{u}|\psi_{i_k}\rangle,$$

for $1 \leq i_1 < \cdots < i_k \leq n$ and $k \geq 0$. The linear map $\wedge \mathbf{u}$ is called the wedged map of \mathbf{u} .

When the linear map \mathbf{u} is of form,

$$\mathbf{u} = \sum_{i,j=1}^n u_{ij} |\psi_i\rangle \langle \psi_j|, \quad (5)$$

the linear operator $U(u; \psi)$ as in (2) is consistent with $\wedge \mathbf{u}$, i.e.,

$$U(u; \psi) = \wedge \mathbf{u}.$$

Appendix A gives the detailed derivation. The derivation gives a proof of Thouless theorem using the language of exterior algebra, which is different from the BCH formula used in Kivlichan *et al.* [11]. We find that the extending linear map $\wedge \mathbf{u}$ to non-unitary transformation is straightforward, whereas extending the operator $U(u; \psi)$ to non-unitary case is more difficult. Hence, the linear map $\wedge \mathbf{u}$ in exterior algebra will be used throughout the rest paper mainly for non-unitary transformations.

An important property of $U(u; \psi)$ is the operator composition property, which builds the foundation for [11]. Precisely, for any two unitary matrices u^1 and u^2 , the composition of $U(u^1; \psi)$ and $U(u^2; \psi)$ is the operator of product of two matrices, i.e.,

$$U(u^1; \psi)U(u^2; \psi) = U(u^1 u^2; \psi). \quad (6)$$

Lemma 2 gives an analog composition property for wedged maps.

Lemma 2. Suppose \mathbf{u}^1 and \mathbf{u}^2 are two linear maps $V \rightarrow V$, then the composition property holds for wedged maps,

$$(\wedge \mathbf{u}^1)(\wedge \mathbf{u}^2) = \wedge(\mathbf{u}^1 \mathbf{u}^2).$$

We emphasize that two linear maps \mathbf{u}^1 and \mathbf{u}^2 in Lemma 2 are not necessary unitary. Lemma 2 holds for non-unitary linear maps as well.

Specifically, we consider two unitary maps defined as,

$$\mathbf{u}^1 = \sum_{i,j=1}^n u_{ij}^1 |\psi_i\rangle \langle \psi_j|, \quad \mathbf{u}^2 = \sum_{i,j=1}^n u_{ij}^2 |\psi_i\rangle \langle \psi_j|.$$

By the equivalence between $U(u; \psi)$ and $\wedge \mathbf{u}$, we have $U(u^1; \psi) = \wedge \mathbf{u}^1$ and $U(u^2; \psi) = \wedge \mathbf{u}^2$. Therefore, the composition of two operators admits,

$$U(u^1 u^2; \psi) = U(u^1; \psi)U(u^2; \psi) = (\wedge \mathbf{u}^1)(\wedge \mathbf{u}^2) = \wedge(\mathbf{u}^1 \mathbf{u}^2).$$

Such a composition property agrees with the composition of maps \mathbf{u}^1 and \mathbf{u}^2 ,

$$\mathbf{u}^1 \mathbf{u}^2 = \sum_{i,j=1}^n (u^1 u^2)_{ij} |\psi_i\rangle \langle \psi_j|,$$

where $u^1 u^2$ denotes the product of two matrices.

Next, we discuss the quantum circuit implementation of $U(u; \psi)$. For general unitary operator in exponent form, e.g., (2), Trotterization is widely adopted in quantum computing, especially in quantum simulation [8, 67]. The Trotterization leads to many number of small time steps and accumulation of truncation errors. For the particular unitary operator $U(u; \psi)$ as in (2), Kivlichan *et al.* [11] proposes a tailored quantum circuit based on Givens QR factorization of u . In the original work [11], real

orthogonal matrix u are considered in detail, and an expression for complex unitary u is provided without detail. In this paper, we revisit and rederive the decomposition for complex unitary matrix u directly. Notably, the final expression is slightly different from that in [11], which should be due to typos therein.

The complex Givens rotation is composed of three parts: two phase rotations and a regular real Givens rotation. The phase rotation acting on the q -th row of a matrix with rotation angle ϕ is denoted as $p_q(\phi) = \text{Diag}\{1, \dots, 1, e^{-i\phi}, 1, \dots, 1\}$, i.e., the identity matrix except the p -th 1 replaced by $e^{-i\phi}$. The regular real Givens rotation by an angle θ between the p -th and q -th rows of a matrix is denoted as $r_{pq}(\theta_{pq})$. Contrast to the regular real Givens rotation, the complex Givens rotation first multiplies the elements to be eliminated by complex signs, i.e., phase rotations, to make them real, and then performs the real Givens rotation. For example, let us consider the case using u_{pi} to eliminate u_{qi} , where both u_{pi} and u_{qi} are complex numbers. The phase rotations, $p_p(\phi_p)$ and $p_q(\phi_q)$, are chosen such that $e^{-i\phi_p}u_{pi} = |u_{pi}|$ and $e^{-i\phi_q}u_{qi} = |u_{qi}|$, respectively. Then the real Givens rotation, $r_{pq}(\theta_{pq})$, is constructed with,

$$\theta_{pq} = \arccos \frac{|u_{pi}|}{\sqrt{|u_{pi}|^2 + |u_{qi}|^2}}.$$

By these constructions, after we multiply $g_{pq} = r_{pq}(\theta_{pq})p_q(\phi_q)p_p(\phi_p)$ to u , the (q, i) entry is zeroed out. Using the complex Givens rotation and regular Givens QR factorization procedure, a unitary matrix u is decomposed as,

$$u = \prod_{pq} g_{pq}^* \cdot \prod_{i=1}^n p_i^*(\phi_i), \quad (7)$$

where

$$g_{pq}^* = p_p(-\phi_p)p_q(-\phi_q)r_{pq}(-\theta_{pq}), \text{ and} \\ p_i^* = p_i(-\phi_i).$$

Notice that there are $\frac{n(n-1)}{2}$ complex Givens rotations in the first product of (7), and the ordering of $\{pq\}$ pairs is not unique. Kivlichan *et al.* [11] propose a specific ordering of $\{pq\}$ to maximize the parallelizability in applying these complex Givens rotations on quantum computer.

By the definition of $U(u; \psi)$, we could define the operation of $U(r_{pq}; \psi)$ and $U(p_p; \psi)$, and denote them, respectively, as

$$\mathbf{R}_{pq}(\theta; \psi) = U(r_{pq}(\theta); \psi), \text{ and} \quad (8) \\ \mathbf{P}_p(\phi; \psi) = U(p_p(\phi); \psi). \quad (9)$$

The corresponding ‘‘complex Givens rotation’’ and its adjoint admit,

$$\mathbf{G}_{pq} = U(g_{pq}) = \mathbf{R}_{pq}(\theta_{pq})\mathbf{P}_q(\phi_q)\mathbf{P}_p(\phi_p), \text{ and} \quad (10) \\ \mathbf{G}_{pq}^* = U(g_{pq}^*) = \mathbf{P}_p(-\phi_p)\mathbf{P}_q(-\phi_q)\mathbf{R}_{pq}(-\theta_{pq}),$$

where we omit ψ , and some θ_{pq} , ϕ_p , ϕ_q for simplicity. Under these notations, the operation $U(u; \psi)$ could be decomposed into many operations of \mathbf{G}_{pq} and \mathbf{P}_i for u defined in (7),

$$U(u; \psi) = \prod_{pq} \mathbf{G}_{pq}^* \prod_{i=1}^n \mathbf{P}_i^*(\phi_i; \psi). \quad (11)$$

Next we demonstrate that the decomposition (11) is sufficiently simple and could be implemented using quantum gates directly. By (2), the explicit expressions of $\mathbf{P}_p = U(p_p(\phi); \psi)$ and $\mathbf{R}_{pq} = U(r_{pq}(\theta); \psi)$ could be written as

$$\mathbf{P}_p(\phi; \psi) = \exp(-i\phi_p \mathbf{n}(\psi_p)), \text{ and} \quad (12) \\ \mathbf{R}_{pq}(\theta; \psi) = \exp[\theta_{pq}(\mathbf{a}^\dagger(\psi_p)\mathbf{a}(\psi_q) - \mathbf{a}^\dagger(\psi_q)\mathbf{a}(\psi_p))], \quad (13)$$

where the detailed derivations could be found in Appendix B.

Now, we turn to the quantum circuit designs for $U(u; \psi)$. To make our discussion rigorous, we make a strict distinction between the quantum state of the physical system being studied and the qubit state in the encoded space of a quantum computer. They are linked to each other by encoded mappings. Here the mapping is the Jordan-Wigner transformation as in Definition 3.

Definition 3. *The Jordan-Wigner transformation of basis $\{|f_i\rangle \mid i = 1, 2, \dots, n\}$ is denoted as J_f , such that:*

$$J_f(|f_{i_1}\rangle \wedge |f_{i_2}\rangle \wedge \dots \wedge |f_{i_k}\rangle) = |n_1 n_2 n_3 \dots\rangle,$$

where $n_1 n_2 n_3 \dots$ is a bit string of length equals to the size of basis set n . And $n_i = 1$ if $i \in \{i_1, i_2, \dots, i_k\}$, $n_i = 0$ otherwise.

These basis vectors $\{|f_i\rangle \mid i = 1, 2, \dots, n\}$ do not need to be a physically meaningful basis, they can be arbitrary abstract basis of any abstract vector space, such as $|f_i\rangle$ is the i -th unit coordinate vector of \mathbb{C}^n . By this definition, the creation and annihilation operators under Jordan-Wigner transformation are the same as the usual definition, i.e.,

$$\mathbf{a}_i^\dagger = J_f \mathbf{a}^\dagger(f_i) J_f^{-1} \\ = Z_1 \otimes \dots \otimes Z_{i-1} \otimes (|1\rangle \langle 0|) \otimes I_{i+1} \otimes \dots \otimes I_n, \text{ and} \\ \mathbf{a}_i = J_f \mathbf{a}(f_i) J_f^{-1} \\ = Z_1 \otimes \dots \otimes Z_{i-1} \otimes (|0\rangle \langle 1|) \otimes I_{i+1} \otimes \dots \otimes I_n. \quad (14)$$

Both ket-bra operations, $|1\rangle \langle 0|$ and $|0\rangle \langle 1|$, are applied to the index i qubit in the above definitions. There is no basis notation in \mathbf{a}_i^\dagger and \mathbf{a}_i because they are operators on qubit states. Basis information are kept in the encoding mapping J_f . This viewpoint is helpful in the section

of inner-product of two states under different bases in Section IV.

Consider a complex Givens rotation, it induces a rotation between rows p and q of the matrix u , allowing for the elimination of a single element in one of those rows. If p and q are not adjacent, the image under Jordan-Wigner transformation of the complex Givens rotation $\mathbf{G}_{pq}(\theta, \phi; \psi)$ will apply gates on all qubits between p and q , which is due to the fact that the Jordan-Wigner transformation of creators and annihilators are non-local. More explicitly, the complex Givens rotation includes terms like $\mathbf{a}^\dagger(\psi_p)\mathbf{a}(\psi_q)$, whose Jordan-Wigner transformation admits,

$$\begin{aligned} & J_\psi(\mathbf{a}^\dagger(\psi_p)\mathbf{a}(\psi_q))J_\psi^{-1} \\ &= Z_1 \otimes \cdots \otimes Z_{p-1} \otimes |1\rangle\langle 0| \otimes \\ & Z_{p+1} \otimes \cdots \otimes Z_{q-1} \otimes |0\rangle\langle 1| \otimes I_{i+1} \otimes \cdots \otimes I_n. \end{aligned}$$

Therefore, if we use the regular Givens QR elimination order, i.e., using the diagonal element to eliminate all the elements below it in its column, it prevents us from applying complex Givens rotations in parallel. In the worst case, it results in a quantum circuit of depth $O(n^2)$ for n being the basis set size. An efficient Givens elimination order is proposed in Kivlichan *et al.* [11] for qubits with linear connectivity. An example with $n = 5$ is depicted in Fig. 1. Through the elimination procedure, the complex Givens rotations are always applied to neighboring rows and eliminate the elements on the second row. The procedure boosts the parallelizability, and $O(n)$ elements, in the best case, are simultaneously eliminated. Using the specific elimination order, it results in a quantum circuit of depth $O(n)$.

$$\begin{pmatrix} * & * & * & * & * \\ 4 & * & * & * & * \\ 3 & 5 & * & * & * \\ 2 & 4 & 6 & * & * \\ 1 & 3 & 5 & 7 & * \end{pmatrix}$$

FIG. 1: Elimination order of elements via complex Givens rotations. The number describes the order that the element been eliminated. Elements with the same number mean that they could be eliminated simultaneously. Asterisks (*) mark all upper-diagonal elements. [11]

We provide an observation that further simplifies the expression of $U(u; \psi)$. After Givens QR upper triangularization, the resulting diagonal matrix typically has all elements equal to 1 except the last bottom-right element. This is due to the phase rotations and unitarity of u . Hence, the $U(u; \psi)$ expression (11) could be rephrased as

$$U(u; \psi) = \prod_i \left[\prod_{q \in \text{Step}_i} (\mathbf{G}_{q-1,q}^{(i)})^* \right] \cdot \mathbf{P}_n^*(\phi_n; \psi). \quad (15)$$

The upper index i of the gate $\mathbf{G}_{q-1,q}^{(i)}$ denotes the i -th step of parallel complex Givens rotations and the set Step_i is

the row indices of the elements eliminated in parallel at the i -th step. Comparing to (11), the product of phase operators is simplified by a single phase operator acting on the n -th row, and parallel sequence of the gates is also indicated. Now we give the quantum circuit of $U(u; \psi)$. Under the Jordan-Wigner transformation with respect to basis $\{|\psi_i\rangle\}_{i=1}^n$, the rotation $\mathbf{R}_{q-1,q}(\theta; \psi)$ is mainly represented by a 4×4 matrix and $\mathbf{R}_{q-1,q}(\theta; \psi)$ is encoded as,

$$\begin{aligned} & J_\psi \mathbf{R}_{q-1,q}(\theta; \psi) J_\psi^{-1} \\ &= I_1 \otimes \cdots \otimes I_{q-2} \otimes \begin{pmatrix} 1 & 0 & 0 & 0 \\ 0 & \cos \theta & -\sin \theta & 0 \\ 0 & \sin \theta & \cos \theta & 0 \\ 0 & 0 & 0 & 1 \end{pmatrix} \otimes \\ & I_{q+1} \otimes \cdots \otimes I_n, \end{aligned} \quad (16)$$

where the middle 4×4 matrix can be expressed as the product of three matrices as,

$$\begin{pmatrix} 1 & 0 & 0 & 0 \\ 0 & 0 & 0 & 1 \\ 0 & 0 & 1 & 0 \\ 0 & 1 & 0 & 0 \end{pmatrix} \cdot \begin{pmatrix} 1 & 0 & 0 & 0 \\ 0 & 1 & 0 & 0 \\ 0 & 0 & \cos \theta & \sin \theta \\ 0 & 0 & -\sin \theta & \cos \theta \end{pmatrix} \cdot \begin{pmatrix} 1 & 0 & 0 & 0 \\ 0 & 0 & 0 & 1 \\ 0 & 0 & 1 & 0 \\ 0 & 1 & 0 & 0 \end{pmatrix}. \quad (17)$$

The first and third matrices in (17) represent the standard quantum CNOT gate, where the first qubit is the target and the second qubit is the control. The second matrix in (17) represents the $\text{CRY}(-2\theta)$ gate, where the first qubit controls the $\text{RY}(-2\theta)$ gate applied to the second qubit. The matrix representation of $\text{RY}(\theta)$ with angle θ is given by

$$\text{RY}(\theta) = \begin{pmatrix} \cos \frac{\theta}{2} & -\sin \frac{\theta}{2} \\ \sin \frac{\theta}{2} & \cos \frac{\theta}{2} \end{pmatrix}.$$

As a result, if we denote the first line as the qubit $q-1$ and the second as the qubit q , we have

$$J_\psi \mathbf{R}_{q-1,q}(\theta; \psi) J_\psi^{-1} = \begin{array}{c} \oplus \\ \text{---} \\ \bullet \\ \text{---} \\ \oplus \end{array} \cdot \begin{array}{c} \text{---} \\ \bullet \\ \text{---} \\ \text{RY}(-2\theta) \\ \text{---} \\ \bullet \\ \text{---} \\ \bullet \\ \text{---} \\ \oplus \end{array}. \quad (18)$$

Then the phase operator is encoded as,

$$\begin{aligned} & J_\psi \mathbf{P}_p(\phi; \psi) J_\psi^{-1} \\ &= I_1 \otimes \cdots \otimes I_{p-1} \otimes \begin{pmatrix} 1 & 0 \\ 0 & e^{-i\phi_p} \end{pmatrix} \otimes I_{p+1} \otimes \cdots \otimes I_n. \end{aligned} \quad (19)$$

In Appendix B, we give the detailed derivations for (16) and (19). The phase operator is simply a phase gate acting on the p -th qubit. Combining the rotation quantum circuit as in (18) together with that of the phase gate, we obtain the quantum circuit for complex Givens rotations applied to adjacent rows, which is denoted as $\mathbf{G}_{q-1,q}^{(i)}$. The overall quantum circuit for $J_\psi U(u; \psi) J_\psi^{-1}$ corresponding to a 5×5 unitary map u is given in Fig. 2. The parallel steps are consistent with that in Fig. 1.

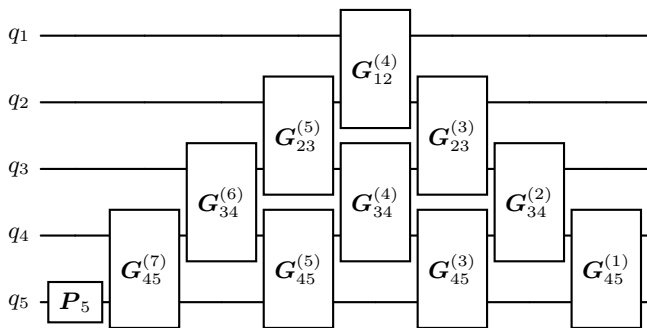


FIG. 2: Quantum circuit for $J_\psi U(u; \psi) J_\psi^{-1}$. All gates are their complex conjugates.

Remark. Comparing to the original work [11], we extend the discussion to complex unitary matrix in detail and provide the corresponding quantum circuit. At the same time, we rewrite some expressions using the exterior algebra notations, which serves as an introduction of notations for our later sections.

III. NON-UNITARY LINEAR TRANSFORMATION

We naturally raise a question: when u is non-unitary, can we extend the linear transformation in Section II? The answer is yes, but the derivation is more complicated and the resulting quantum circuit is about twice the depth of the unitary one. There are at least two potential applications for the non-unitary linear transformation: a) calculating the overlap between two states under different bases, which is detailed in the next section; b) change of basis to a non-orthogonal one.

As we mentioned earlier, the Thouless theorem in (2) form is too difficult to be extended to non-unitary case, which is mainly due to the logarithm of a non-unitary matrix. Hence, we stick to exterior algebra representation of Thouless theorem and all later derivations are in the language of exterior algebra. We recall the notation we use, i.e., $U(u; \psi)$ and $\wedge \mathbf{u}$. When u is a unitary matrix, two operators are equal $U(u; \psi) = \wedge \mathbf{u}$, for $U(u; \psi)$, $\wedge \mathbf{u}$ and \mathbf{u} being defined in (2), Definition 1, and (5), respectively. When u is non-unitary, we use $\wedge \mathbf{u}$ for the linear map and avoid using $U(u; \psi)$.

In order to reduce the overall circuit depth for the non-unitary linear transformation, our construction relies on the singular value decomposition (SVD) of u and hence its operator \mathbf{u} . Let the SVD of a non-unitary matrix u be of form,

$$u = LDR,$$

where L and R are left and right singular vectors, $D = \text{diag}(\sigma_1, \dots, \sigma_n)$ is a diagonal matrix with singular values in non-increasing ordering, i.e., $\sigma_1 \geq \dots \geq \sigma_n$. Without loss of generality, we further assume that u is

a nonunitary matrix with 2-norm bounded by one, i.e., $1 \geq \sigma_1 \geq \dots \geq \sigma_n$. Singular vectors L and R are unitary matrices. Let $\{|\psi_i\rangle\}_{i=1}^n$ be the set of underlying basis set. The operator \mathbf{u} associated with u also admits an operator SVD,

$$\mathbf{u} = LDR, \quad (20)$$

where L , D , and R are associated with matrices L , D , and R respectively,

$$\begin{aligned} L &= \sum_{i,j=1}^n L_{ij} |\psi_i\rangle \langle \psi_j|, \\ D &= \sum_{i=1}^n \sigma_i |\psi_i\rangle \langle \psi_i|, \text{ and} \\ R &= \sum_{i,j=1}^n R_{ij} |\psi_i\rangle \langle \psi_j|. \end{aligned}$$

By Lemma 2, we have $\wedge \mathbf{u} = (\wedge L)(\wedge D)(\wedge R)$. For unitary matrices L and R , the operators $\wedge L = U(L; \psi)$ and $\wedge R = U(R; \psi)$ can be implemented by quantum circuits as in Section II, e.g., analog quantum circuits of Fig. 2. In the following, we focus on the quantum circuit construction for the wedged diagonal operator $\wedge D$.

We first rewrite $\wedge D$ as a composition of at most n simple operators, which are simple to be implemented by quantum gates. According to Definition 1, the action of $\wedge D$ on an exterior algebra is defined as applying the operator D to all one-body states, as,

$$\begin{aligned} (\wedge D) |\psi_{i_1}\rangle \wedge |\psi_{i_2}\rangle \wedge \dots \wedge |\psi_{i_k}\rangle \\ = D |\psi_{i_1}\rangle \wedge D |\psi_{i_2}\rangle \wedge \dots \wedge D |\psi_{i_k}\rangle \\ = \sigma_{i_1} \sigma_{i_2} \dots \sigma_{i_k} |\psi_{i_1}\rangle \wedge |\psi_{i_2}\rangle \wedge \dots \wedge |\psi_{i_k}\rangle. \end{aligned} \quad (21)$$

It is worth noting that this expression is closely related to the particle number operator. It acts like a weighted number operator. More explicitly, if the many-body state includes the state $|\psi_i\rangle$, the result of the operation will give a factor σ_i . Thus, we define an operator

$$\boldsymbol{\nu}(\psi_j) = \mathbf{1} + (\sigma_j - 1)\mathbf{n}(\psi_j),$$

which admits,

$$\begin{aligned} \boldsymbol{\nu}(\psi_j) (|\psi_{i_1}\rangle \wedge |\psi_{i_2}\rangle \wedge \dots \wedge |\psi_{i_k}\rangle) \\ = \begin{cases} \sigma_j (|\psi_{i_1}\rangle \wedge |\psi_{i_2}\rangle \wedge \dots \wedge |\psi_{i_k}\rangle), & j \in \{i_1, i_2, \dots, i_k\} \\ |\psi_{i_1}\rangle \wedge |\psi_{i_2}\rangle \wedge \dots \wedge |\psi_{i_k}\rangle, & j \notin \{i_1, i_2, \dots, i_k\} \end{cases} \end{aligned}$$

Here $\mathbf{n}(\psi_j) = \mathbf{a}^\dagger(\psi_j)\mathbf{a}(\psi_j)$ is the number operator. Next, we justify that the wedge operator $\wedge D$ is equivalent to the composition of $\boldsymbol{\nu}(\psi_j)$. For any basis $|\psi_{i_1}\rangle \wedge \dots \wedge |\psi_{i_k}\rangle$ in the exterior algebra (Fock space), the action of the composition of $\boldsymbol{\nu}(\psi_j)$ admits,

$$\begin{aligned} \left(\prod_{j=1}^n \boldsymbol{\nu}(\psi_j) \right) |\psi_{i_1}\rangle \wedge |\psi_{i_2}\rangle \wedge \dots \wedge |\psi_{i_k}\rangle \\ = \sigma_{i_1} \sigma_{i_2} \dots \sigma_{i_k} |\psi_{i_1}\rangle \wedge |\psi_{i_2}\rangle \wedge \dots \wedge |\psi_{i_k}\rangle \end{aligned}$$

which equals (21). Hence, we conclude that the product operator $\prod_{j=1}^n \nu(\psi_j)$ is another form of $\wedge \mathbf{D}$, i.e.,

$$\wedge \mathbf{D} = \prod_{j=1}^n \nu(\psi_j).$$

Now we move on to the quantum circuit implementation of composed operator $\wedge \mathbf{D} = \prod_{j=1}^n \nu(\psi_j)$. Obviously, $\nu(\psi_j)$ is not a unitary operator, and hence, cannot be implemented by quantum circuits directly. We introduce an ancilla qubit to encode the action of $\nu(\psi_j)$. In the context of the Jordan-Wigner transformation, the particle number operator admits,

$$\mathbf{n}_j = I_1 \otimes \cdots \otimes I_{j-1} \otimes \begin{pmatrix} 0 & 0 \\ 0 & 1 \end{pmatrix} \otimes I_{j+1} \otimes \cdots \otimes I_n.$$

We define an operator acting on qubit state as ν_j admitting,

$$\begin{aligned} \nu_j &= J_\psi \nu(\psi_j) J_\psi^{-1} \\ &= I_1 \otimes \cdots \otimes I_{j-1} \otimes \begin{pmatrix} 1 & 0 \\ 0 & \sigma_j \end{pmatrix} \otimes I_{j+1} \otimes \cdots \otimes I_n, \end{aligned}$$

where the operator norm is bounded by 1 and so is σ_j .

We divide the discussion of quantum circuit implementation of ν_j into three cases: $\sigma_j = 1$, $0 < \sigma_j < 1$, and $\sigma_j = 0$. For simplicity, we drop the subscript j in the following discussion.

When $\sigma = 1$, the corresponding operator ν is an identity operator, which does not require any quantum gates and any ancilla qubit.

When $0 < \sigma < 1$, the corresponding operator ν is nonunitary. To incorporate this operation into a quantum circuit, we adopt an extra ancilla qubit. The particular block encoding we use for the 2-by-2 matrix in ν admits,

$$\begin{aligned} \tilde{\nu} &= \begin{pmatrix} 1 & 0 & 0 & 0 \\ 0 & \sigma & 0 & -\sqrt{1-\sigma^2} \\ 0 & 0 & 1 & 0 \\ 0 & \sqrt{1-\sigma^2} & 0 & \sigma \end{pmatrix} \\ &= \begin{pmatrix} 1 & 0 & 0 & 0 \\ 0 & \cos \frac{\theta}{2} & 0 & -\sin \frac{\theta}{2} \\ 0 & 0 & 1 & 0 \\ 0 & \sin \frac{\theta}{2} & 0 & \cos \frac{\theta}{2} \end{pmatrix}, \end{aligned}$$

where the first qubit is the ancilla qubit and the second one is the working qubit, and $\theta = 2 \arccos \sigma$. This encoded matrix $\tilde{\nu}$ on 2-qubit is the controlled-RY gate, denoted as CRY(θ). This controlled-RY gate applies a rotation around the Y-axis by an angle θ to the ancilla qubit and controlled by the working qubit. Denote P_a as the projection operator that project the ancilla qubit to $|0\rangle$ state, which could be implemented via a measurement, then the construction $\tilde{\nu}$ satisfies

$$P_a \tilde{\nu} |0\rangle \otimes |\alpha\rangle = |0\rangle \otimes \nu |\alpha\rangle.$$

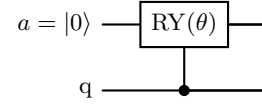


FIG. 3: Quantum circuit of embedded 2-qubit gate. Ancilla qubit is denoted as a , which is initialized to $|0\rangle$ state. The second qubit q is the working qubit which ν is acted on.

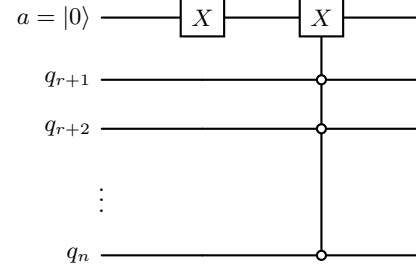


FIG. 4: Block encoding for all ν_j with $\sigma_j = 0$. Here the ancilla qubit a is initialized to $|0\rangle$ state. Other q_j for $r < j \leq n$ are working qubits corresponding to zero singular values of u .

The quantum circuit for $\tilde{\nu}$ is given in Fig. 3.

The last case is that $\sigma = 0$. The technique used for $0 < \sigma < 1$ case applies to the $\sigma = 0$ case as well. Then for each $\tilde{\nu}_j$ with singular value $\sigma_j = 0$, we need an ancilla qubit. Instead, we implement the quantum circuit for all $\sigma = 0$ together and use only one ancilla qubit to perform the block encoding.

Let $r = \arg \max_i \{\sigma_i > 0\}$ be the rank of the nonunitary matrix u . Then we have $\sigma_i > 0$ for $i = 1, \dots, r$ and $\sigma_i = 0$ for $i = r + 1, \dots, n$. Noting that ν_j with $\sigma_j = 0$ is the projection that projects qubit q_j onto $|0\rangle$ state. Thus, the composition of operators

$$\prod_{i=r+1}^n \nu_i$$

is the projection that projects qubits indexed from $r + 1$ to n to $|0 \cdots 0\rangle$. It can be implemented as a X gate combined with a multi-open-controlled Toffoli gate. More specifically, given an ancilla qubit at state $|0\rangle$ and working qubits q_{r+1}, \dots, q_n , we first flip the ancilla qubit to state $|1\rangle$ via an X gate. Then targeting the ancilla qubit, we apply a multi-open-controlled Toffoli gate controlled from all working qubits q_{r+1}, \dots, q_n . Open-controlled gate means that the gate is applied only if the controlling qubits are in state $|0 \cdots 0\rangle$. After these two gates, the quantum state will be linear combination of

$$|0\rangle |0 \cdots 0\rangle \quad \text{and} \quad |1\rangle |0 \cdots 0\rangle_{\perp},$$

where the first qubit is ancilla, the rest are working qubits q_{r+1}, \dots, q_n , and $|0 \cdots 0\rangle_{\perp}$ is a state perpendicular to

$|0 \cdots 0\rangle$). Hence, applying a measurement with selected result, i.e., projecting the ancilla qubit to $|0\rangle$, will turn all working qubits q_{r+1}, \dots, q_n to state $|0\rangle$. Thus, such a quantum circuit is the block encoding as we need. This scheme reduces the number of ancilla qubits down to one for low-rank linear transformations u . However, the actual quantum circuit depth in implementing the multi-open-controlled Toffoli gate depends on the underlying quantum computer hardware, which is beyond the scope of this paper. Figure 4 illustrates the detailed quantum circuit for the case $\sigma = 0$.

As discussed above, both cases $\sigma = 1$ and $\sigma = 0$ lead to more quantum resource efficient circuit implementation than that of case $0 < \sigma < 1$. Hence, naturally, we consider rounding up some large singular values to one and truncating some small singular values to zero. Although both rounding up and truncating reduce the quantum resource cost, both of them would introduce approximation errors. Denote the modification on the j -th singular values as ϵ_j . The approximation error introduced by both the rounding-up and truncating could be bounded as,

$$\left\| \otimes_{j=1}^n \begin{pmatrix} 1 & 0 \\ 0 & \sigma_j + \epsilon_j \end{pmatrix} - \otimes_{j=1}^n \begin{pmatrix} 1 & 0 \\ 0 & \sigma_j \end{pmatrix} \right\| \leq \sum_{j=1}^n \epsilon_j,$$

where the matrix 2-norm is used. Let \tilde{u} denote the matrix that shares the same singular vectors as u , but has rounded up or truncated singular values, i.e., $\tilde{u}_{ij} = \sum_{k=1}^n \tilde{\sigma}_k L_{ik} R_{kj} = \sum_{k=1}^n (\sigma_k + \epsilon_k) L_{ik} R_{kj}$. In this context, the error of approximated wedge operator can be bounded more concisely as,

$$\|\wedge \mathbf{u} - \wedge \tilde{\mathbf{u}}\| \leq \sum_{j=1}^n \epsilon_j. \quad (22)$$

Therefore, the overall approximation error could be well-controlled if all ϵ_j s are small.

Finally, we assemble all above techniques together and propose the quantum circuit construction of a non-unitary linear transformation $\wedge \mathbf{u}$. To incorporate the rounding-up and truncating techniques, we introduce a threshold ϵ . The quantum circuit for the non-unitary linear transformation $\wedge \mathbf{u}$ can be approximately implemented as follows.

1. Calculate the SVD of u , i.e., $u_{ij} = \sum_{k=1}^n \sigma_k L_{ik} R_{kj}$, with singular values σ_i s in non-increasing ordering.
2. Round up large singular values of u and truncate small singular values of u , i.e.,

$$\tilde{\sigma}_i = \begin{cases} 1 & \sigma_i \geq 1 - \epsilon \\ \sigma_i & \epsilon < \sigma_i < 1 - \epsilon \\ 0 & \sigma_i \leq \epsilon \end{cases}.$$

Let the number of $\tilde{\sigma}_i = 1$ be s and the rank after truncation be r .

3. Prepare $r - s + 1$ ancilla qubits to state $|0\rangle$, denote them as $a_{s+1}, a_{s+1}, \dots, a_{r+1}$.

4. Apply the unitary operator $J_\psi U(R; \psi) J_\psi^{-1}$ to the n working qubits following the circuit construction in Section II.
5. Apply controlled-RY gates controlling from q_i targeting a_i for $i = s + 1, \dots, r$.
6. Apply an X gate to flip ancilla qubit a_{r+1} and then apply a multi-open-controlled Toffoli gate controlling from q_{r+1}, \dots, q_n targeting a_{r+1} .
7. Apply the unitary operator $J_\psi U(L; \psi) J_\psi^{-1}$ to the n working qubits following the circuit construction in Section II.
8. Project all ancilla qubits to $|0\rangle$ state via measurement and post-selection.

In Fig. 5, we provide the quantum circuit for a non-unitary matrix u of dimension 8. After the rounding-up and truncating, the approximated non-unitary matrix has 2 singular values equal to 1 and of rank 5.

Remark. If we remove step 8 and stop at step 7, we actually obtain the quantum circuit corresponding to the block encoding of $\wedge \mathbf{u}$. Block-encoding is a standard framework used to embed non-unitary matrices into unitary matrices, allowing them to be implemented as quantum circuits along with some measurements [68]. In the next section, we will discuss how to use the block-encoding we provided here in the context of calculating inner products.

The quantum circuit depth and the number of gates can be estimated based on the matrix dimension n , approximated number of ones s and approximated rank r . The dimension of L and R are both n . And the numbers of gates, as in Section II for the unitary case, are bounded by $\frac{n^2}{2} + O(n)$ rotation gates (18) and $n^2 + O(n)$ phase gates. When qubits are assumed to be linearly connected, the circuit depths for L and R are bounded by $O(n)$ times the rotation gate depth. The number of gates for the $\prod_{k=1}^n \nu_k$ part depends on the gate counting of the multi-open-controlled Toffoli gate. The quantum circuit for the singular value part costs $r - s + 2$ simple gates and one multi-open-controlled Toffoli gate. The circuit depth is bounded by that of the multi-open-controlled Toffoli gate. Applying the standard decomposition as in [8], an additional ancilla qubit is used, and the quantum circuit depth is $O((n - r)^2)$ for $n - r$ being the number of controlling qubits. Overall, the total quantum circuit depth is bounded by $O((n - r)^2 + n)$.

IV. INNER PRODUCT: AN APPLICATION

We consider two sets of one-body bases, $\{|\psi_i\rangle\}_{i=1}^n$ and $\{|\phi_j\rangle\}_{j=1}^n$. The inner products between all pairs of bases $|\psi_i\rangle$ and $|\phi_j\rangle$ are available and denoted as u_{ij} , i.e., $u_{ij} = \langle \psi_i | \phi_j \rangle$, for $1 \leq i, j \leq n$. For the sake of notation, we assume two bases are of the same dimension n . Our proposed algorithm could be easily extended to two

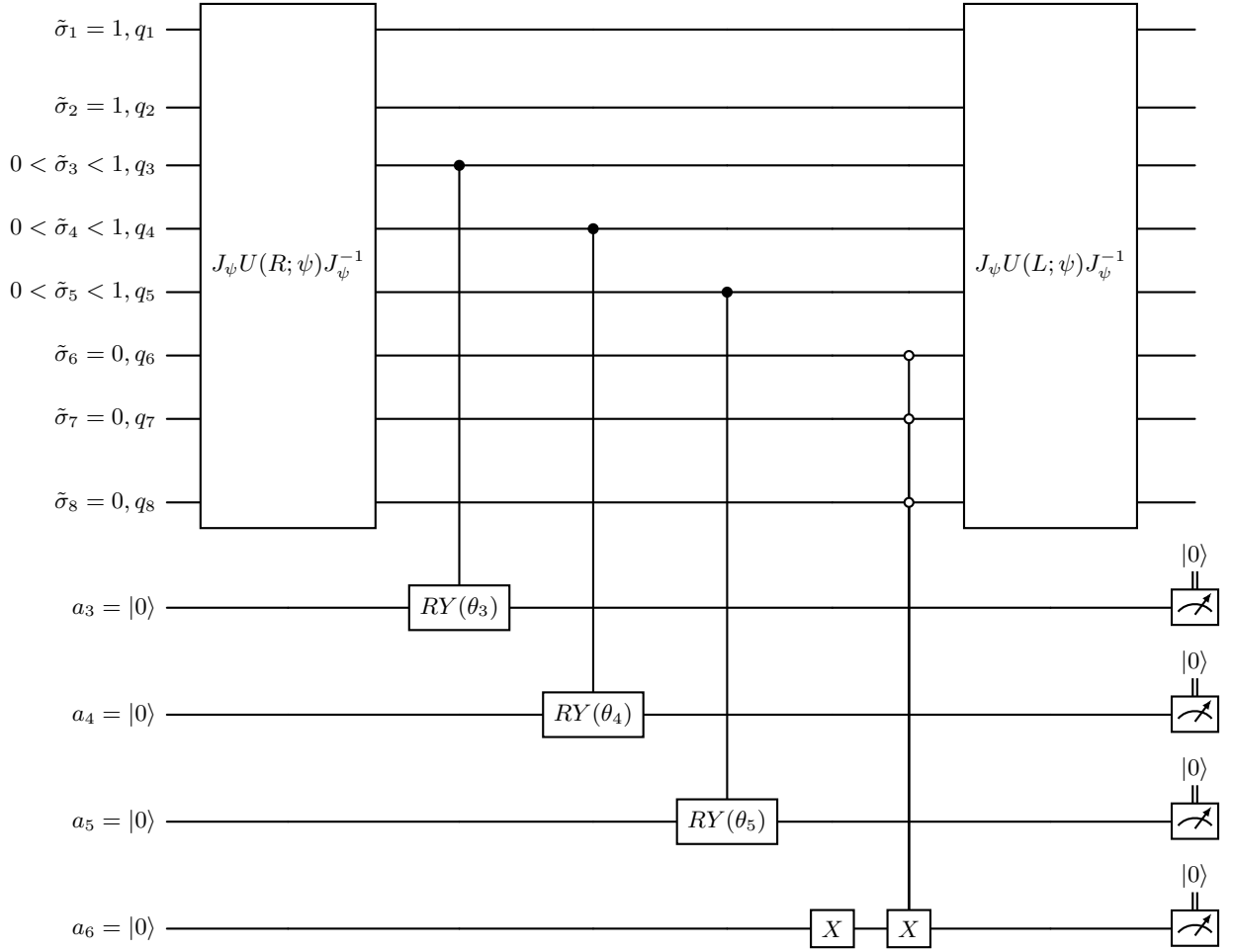


FIG. 5: An example for a nonunitary matrix u of dimension 8 with approximated singular values $\tilde{\sigma}_1 = \tilde{\sigma}_2 = 1$, $1 > \tilde{\sigma}_3 \geq \tilde{\sigma}_4 \geq \tilde{\sigma}_5 > 0$, and $\tilde{\sigma}_6 = \tilde{\sigma}_7 = \tilde{\sigma}_8 = 0$. This quantum circuit is the approximated block encoding of $\wedge u$.

bases of different dimensions. Two many-body states are denoted as $|\Psi\rangle$ and $|\Phi\rangle$, i.e.,

$$|\Psi\rangle = \sum_{1 \leq i_1 < i_2 < \dots < i_k \leq n} c_{i_1 i_2 \dots i_k} |\psi_{i_1}\rangle \wedge |\psi_{i_2}\rangle \wedge \dots \wedge |\psi_{i_k}\rangle,$$

$$|\Phi\rangle = \sum_{1 \leq i_1 < i_2 < \dots < i_k \leq n} c'_{i_1 i_2 \dots i_k} |\phi_{i_1}\rangle \wedge |\phi_{i_2}\rangle \wedge \dots \wedge |\phi_{i_k}\rangle.$$

We consider the scenario such that both many-body states are already encoded and prepared in quantum computer, where these states might be generated from ansatz circuits used in VQE framework, from quantum simulations, or initial state preparation methods. The encoded many-body states on quantum computer are denoted as,

$$|\Psi^q\rangle = \sum_{I=0}^{2^n-1} d_I |I\rangle, \quad \text{and} \quad |\Phi^q\rangle = \sum_{I=0}^{2^n-1} d'_I |I\rangle,$$

where $|I\rangle$ is a bit string representing states on quantum computer. States $|\Psi\rangle$ and $|\Psi^q\rangle$ are connected via a quan-

tum encoding or transformation \mathbf{Q}_ψ , where the subscript ψ indicates that the encoding is related to basis $\{|\psi_i\rangle\}_{i=1}^n$. Similarly, states $|\Phi\rangle$ and $|\Phi^q\rangle$ are connected via \mathbf{Q}_ϕ . More precisely, the connections admit,

$$\mathbf{Q}_\psi |\Psi\rangle = |\Psi^q\rangle, \quad \text{and} \quad \mathbf{Q}_\phi |\Phi\rangle = |\Phi^q\rangle.$$

When Jordan-Wigner encoding is adopted, \mathbf{Q}_ψ is the same as J_ψ . Here, we use \mathbf{Q}_ψ as the encoding map to include other encodings, e.g., parity encoding, Bravyi-Kitaev encoding, etc.

When two basis sets are the same and the encoding is also the same and unitary, the inner product between two states $|\Psi\rangle$ and $|\Phi\rangle$ is the same as that of two states on quantum computer, i.e.,

$$\langle \Phi | \Psi \rangle = \langle \Phi^q | \Psi^q \rangle.$$

Then, we could use many standard quantum circuits to evaluate it or its modulus. A commonly used one is the swap test as in Fig. 6. Other choices are also widely used

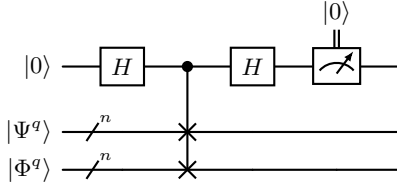


FIG. 6: Swap test circuit to calculate the modulus of the inner-product $|\langle \Phi^q | \Psi^q \rangle|$. The modulus square $|\langle \Phi^q | \Psi^q \rangle|^2$ equals to the probability of the measurement result being $|0\rangle$.

in excited state calculations [40, 69]. However, when two states $|\Psi\rangle$ and $|\Phi\rangle$ are under different basis sets, none of the aforementioned quantum circuits for $\langle \Phi^q | \Psi^q \rangle$ can be used directly, due to the fact that $\langle \Phi | \Psi \rangle \neq \langle \Phi^q | \Psi^q \rangle$.

Notice that the inner product of two states is of a bilinear form. Without loss of generality, we analyze the case that both many-body states are many-body standard basis states, i.e.,

$$\begin{aligned} |\Psi\rangle &= |\psi_{i_1}\rangle \wedge |\psi_{i_2}\rangle \wedge \cdots \wedge |\psi_{i_k}\rangle, \\ |\Phi\rangle &= |\phi_{j_1}\rangle \wedge |\phi_{j_2}\rangle \wedge \cdots \wedge |\phi_{j_k}\rangle. \end{aligned}$$

Further, we introduce an auxiliary basis $\{|\omega_i\rangle\}_{i=1}^n$ to facilitate the calculations. Note that the auxiliary basis will not affect the results and its choice is arbitrary. We could choose it to be any orthonormal basis in \mathbb{C}^n . The auxiliary space spanned by $\{|\omega_i\rangle\}_{i=1}^n$ is denoted as Ω . A linear map $\mathbf{u} : \Omega \rightarrow \Omega$ is defined as

$$\mathbf{u} = \sum_{i,j=1}^n \langle \psi_i | \phi_j \rangle |\omega_i\rangle \langle \omega_j|. \quad (23)$$

Using the linear map \mathbf{u} , the inner product of $|\Psi\rangle$ and $|\Phi\rangle$ admits,

$$\begin{aligned} \langle \Phi | \Psi \rangle &= \langle \psi_{i_1}\rangle \wedge \cdots \wedge \langle \psi_{i_k}\rangle, \langle \phi_{j_1}\rangle \wedge \cdots \wedge \langle \phi_{j_k}\rangle \rangle \\ &= \det \begin{pmatrix} \langle \psi_{i_1} | \phi_{j_1} \rangle & \cdots & \langle \psi_{i_1} | \phi_{j_k} \rangle \\ \vdots & \ddots & \vdots \\ \langle \psi_{i_k} | \phi_{j_1} \rangle & \cdots & \langle \psi_{i_k} | \phi_{j_k} \rangle \end{pmatrix} \\ &= \det \begin{pmatrix} \langle \omega_{i_1} | \mathbf{u} | \omega_{j_1} \rangle & \cdots & \langle \omega_{i_1} | \mathbf{u} | \omega_{j_k} \rangle \\ \vdots & \ddots & \vdots \\ \langle \omega_{i_k} | \mathbf{u} | \omega_{j_1} \rangle & \cdots & \langle \omega_{i_k} | \mathbf{u} | \omega_{j_k} \rangle \end{pmatrix} \\ &= \langle \omega_{i_1}\rangle \wedge \cdots \wedge \langle \omega_{i_k}\rangle, \mathbf{u} | \omega_{j_1}\rangle \wedge \cdots \wedge \mathbf{u} | \omega_{j_k}\rangle \rangle \\ &= \langle \omega_{i_1}\rangle \wedge \cdots \wedge \langle \omega_{i_k}\rangle, \wedge \mathbf{u} | \omega_{j_1}\rangle \wedge \cdots \wedge \mathbf{u} | \omega_{j_k}\rangle \rangle. \end{aligned} \quad (24)$$

Recall that Q_ψ , Q_ϕ , and Q_ω are the same quantum encoding technique applied to different basis sets. Hence, for two many-body bases constructed by the same selection of one-body bases, their quantum encoding map to the same state representation on quantum computer, i.e., the same bit string representation. More precisely,

for two many-body bases, $|\psi_{i_1}\rangle \wedge |\psi_{i_2}\rangle \wedge \cdots \wedge |\psi_{i_k}\rangle$ and $|\omega_{i_1}\rangle \wedge |\omega_{i_2}\rangle \wedge \cdots \wedge |\omega_{i_k}\rangle$, which are constructed by one-body bases of the same indices i_1, i_2, \dots, i_k , their quantum encoded states are the same, i.e.,

$$Q_\psi(|\psi_{i_1}\rangle \wedge |\psi_{i_2}\rangle \wedge \cdots \wedge |\psi_{i_k}\rangle) = Q_\omega(|\omega_{i_1}\rangle \wedge |\omega_{i_2}\rangle \wedge \cdots \wedge |\omega_{i_k}\rangle).$$

Using such a relationship of quantum encoding, we continue deriving (24) as,

$$\begin{aligned} \langle \Phi | \Psi \rangle &= \langle \omega_{i_1}\rangle \wedge \cdots \wedge \langle \omega_{i_k}\rangle, \wedge \mathbf{u} | \omega_{j_1}\rangle \wedge \cdots \wedge \mathbf{u} | \omega_{j_k}\rangle \rangle \\ &= \langle Q_\omega^{-1} Q_\omega | \omega_{i_1}\rangle \wedge \cdots \wedge \langle \omega_{i_k}\rangle, \\ &\quad \langle \wedge \mathbf{u} Q_\omega^{-1} Q_\omega | \omega_{j_1}\rangle \wedge \cdots \wedge \langle \omega_{j_k}\rangle \rangle \\ &= \langle Q_\omega^{-1} Q_\psi | \psi_{i_1}\rangle \wedge \cdots \wedge \langle \psi_{i_k}\rangle, \\ &\quad \langle \wedge \mathbf{u} Q_\omega^{-1} Q_\phi | \phi_{j_1}\rangle \wedge \cdots \wedge \langle \phi_{j_k}\rangle \rangle \\ &= \langle Q_\omega^{-1} | \Psi^q \rangle, \langle \wedge \mathbf{u} Q_\omega^{-1} | \Phi^q \rangle \rangle. \end{aligned} \quad (25)$$

Notice that the quantum encoding map Q_ω preserves the inner-product, i.e.,

$$\begin{aligned} \langle Q_\omega | \omega_{i_1}\rangle \wedge \cdots \wedge \langle \omega_{i_k}\rangle, Q_\omega | \omega_{j_1}\rangle \wedge \cdots \wedge \langle \omega_{j_k}\rangle \rangle \\ = \langle |\omega_{i_1}\rangle \wedge \cdots \wedge \langle \omega_{i_k}\rangle, |\omega_{j_1}\rangle \wedge \cdots \wedge \langle \omega_{j_k}\rangle \rangle, \end{aligned}$$

for any ω , and i_1, \dots, i_k , and j_1, \dots, j_k . Therefore, in the last expression in (25), we could multiply both side by Q_ω and obtain the definition of operator $\Xi(\psi, \phi)$,

$$\langle \Phi | \Psi \rangle = \langle | \Psi^q \rangle, Q_\omega (\wedge \mathbf{u} Q_\omega^{-1} | \Phi^q \rangle) \rangle = \langle \Psi^q | \Xi(\psi, \phi) | \Phi^q \rangle, \quad (26)$$

where

$$\Xi(\psi, \phi) = Q_\omega (\wedge \mathbf{u} Q_\omega^{-1}).$$

In (26), both $|\Phi^q\rangle$ and $|\Psi^q\rangle$ are quantum encoded states, which are constructed by their own quantum circuits. The remaining task in evaluating the inner product $\langle \Phi | \Psi \rangle$ is to construct $\Xi(\psi, \phi)$ as a quantum circuit. From now on, we take Q_ω here as the Jordan-Wigner mapping J_ω such that the quantum circuits in Section II and Section III could be reused directly. Then, the quantum circuit for $\Xi(\psi, \phi)$ is exactly the same as that proposed in Section III with $u_{ij} = \langle \psi_i | \phi_j \rangle$ and $\{|\omega_i\rangle\}_{i=1}^n$ being the underlying basis set. More precisely, incorporating the quantum circuit for $\Xi(\psi, \phi)$ as illustrated in Fig. 5 and projecting all ancilla qubits to state $|0\rangle$, we could obtain the quantum state $\Xi(\psi, \phi) | \Phi^q \rangle$ on quantum computer. For a better understanding and comparison between different inner product quantum circuits, we denote $\tilde{\Xi}(\psi, \phi)$ as the block encoding of $\Xi(\psi, \phi)$. For example, for $\Xi(\psi, \phi)$ in Fig. 5, $\tilde{\Xi}(\psi, \phi)$ is the quantum circuit therein without projecting ancilla qubits to $|0\rangle$.

Combining the quantum circuit for $\Xi(\psi, \phi)$ and swap test as in Fig. 6, we obtain our first quantum circuit for $|\langle \Psi | \Phi \rangle|$ as in Fig. 7. Notice that in Fig. 7, the quantum circuit is constructed using $\tilde{\Xi}(\psi, \phi)$ and all measurements are postponed to the end and been measured simultaneously. This quantum circuit only require one extra ancilla

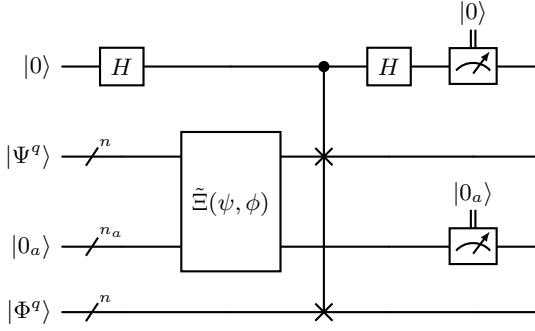


FIG. 7: Swap test circuit to calculate the inner-product $|\langle\Phi|\Psi\rangle|$. The absolute value square $|\langle\Phi|\Psi\rangle|^2$ is the probability of all the measurement being $|0\rangle$.

qubit for inner product. Instead, we need to measure all ancilla qubits, including those from $\Xi(\psi, \phi)$ and the one from swap test. The probability of $a + 1$ ancilla qubits in $|0\rangle$ leads to the absolute value of the desired inner product, $|\langle\Psi|\Phi\rangle|$. Slightly modified quantum circuits could be used to evaluate the real and imaginary part of $\langle\Psi|\Phi\rangle$, and lead to the value of the desired inner product.

The quantum circuit in Fig. 7 evaluates the absolute value of the inner product based on the following equation,

$$\langle\Psi|\Phi\rangle = \langle\Psi^q|\Xi(\psi, \phi)|\Phi^q\rangle = \langle\Psi^q|\langle 0_a|\tilde{\Xi}(\psi, \phi)|\Phi^q\rangle|0_a\rangle, \quad (27)$$

where $|0_a\rangle$ denotes the ancilla qubits in the block encoding of $\Xi(\psi, \phi)$. In Fig. 7, the inner product with $\langle 0_a|$ is carried out by the measurement and the inner product with $\langle\Psi^q|$ is carried out by the swap test.

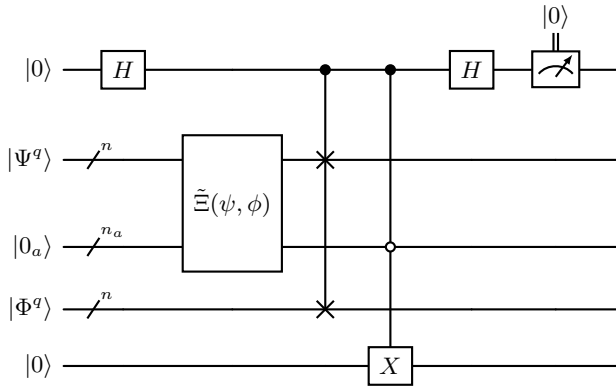


FIG. 8: Alternative swap test circuit to calculate the inner-product $|\langle\Phi|\Psi\rangle|$. The absolute value square $|\langle\Phi|\Psi\rangle|^2$ is the probability of the ancilla measurement being $|0\rangle$.

In some cases, measurements are not favored, e.g., the measurement errors are large. Instead of the quantum circuit in Fig. 7, we could propose other quantum circuits

to evaluate the inner product as well.

An alternative quantum circuit for the inner product is to evaluate both inner products with $\langle 0_a|$ and $\langle\Psi^q|$ in (27) using swap test. In this case, only one measurement is needed, while extra a ancilla qubits are required for $\langle 0_a|$. In fact, we can simplify such a quantum circuit, replacing the extra a ancilla qubits by a single ancilla qubit and replacing the controlled swap gates between ancilla qubits by a multi-controlled NOT gate. The simplified quantum circuit is given in Fig. 8.

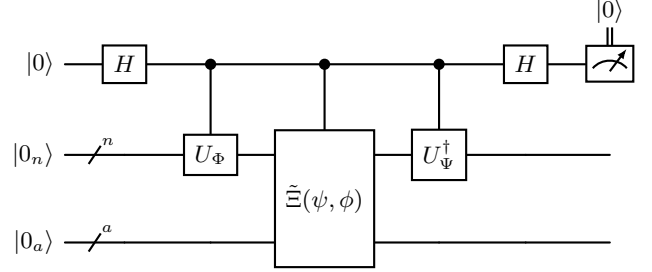


FIG. 9: Hadamard test circuit to calculate $\text{Re}\langle\Psi|\Phi\rangle$, which could be inferred from the probabilities of the measurement result.

Another alternative quantum circuit for the inner product is based on the Hadamard test. Here we consider a slightly different setting. Suppose that we have quantum circuits U_Ψ and U_Φ for preparing states $|\Psi^q\rangle$ and $|\Phi^q\rangle$, respectively, i.e.,

$$|\Psi^q\rangle = U_\Psi|0_n\rangle, \text{ and } |\Phi^q\rangle = U_\Phi|0_n\rangle.$$

Under the VQE framework, U_Ψ and U_Φ are known from parameterized ansatz quantum circuits. Then, the inner product admits,

$$\begin{aligned} \langle\Phi|\Psi\rangle &= \langle\Psi^q|\langle 0_a|\tilde{\Xi}(\psi, \phi)|\Phi^q\rangle|0_a\rangle \\ &= \langle 0_{n+a}|(U_\Psi^\dagger \otimes I_a)\tilde{\Xi}(\psi, \phi)(U_\Phi \otimes I_a)|0_{n+a}\rangle. \end{aligned}$$

The quantum circuit to evaluate the real part of $\langle\Phi|\Psi\rangle$ is given in Fig. 9, where the controlled- $(U_\Psi^\dagger \otimes I_a)$ and controlled- $(U_\Phi \otimes I_a)$ are simplified by the controlled- U_Ψ^\dagger and controlled- U_Φ respectively. A simple modification leads to the quantum circuit for the imaginary part of $\langle\Psi|\Phi\rangle$. When the adjoint of the ansatz circuit is not favored, inner product quantum circuits proposed in [69] could be used as an alternative to the Hadamard test.

V. SUMMARY

This paper proposes a novel quantum circuit design for non-unitary linear transformations of basis sets. The non-unitary linear transformations of basis sets could be used in many practical scenarios, including but not limited to the change of basis in initial state preparation,

evaluating the overlapping between two states under different basis sets in excited state calculation under the VQE framework, etc.

Let \mathbf{u} be a non-unitary linear transformation of one-body basis sets, $\mathbf{u} : V \rightarrow V$ for V being the space spanned by one-body bases. The designed quantum circuit implements the wedged map on the exterior algebra of V (Fock Space), i.e., $\wedge \mathbf{u} : \wedge V \rightarrow \wedge V$. To reduce the overall circuit complexity, we first calculate an SVD of \mathbf{u} . The left and right singular vector operators of \mathbf{u} are unitary and are implemented by the unitary linear transformation proposed in [11], which is reviewed in Section II. The quantum circuit for the singular values of \mathbf{u} are detailed in Section III. Block encodings are applied to all singular values strictly between zero and one. The same block encoding could be applied to zero singular value as well. Instead, we propose a quantum circuit to encoding all zero singular values together with only one extra ancilla qubit. For singular values that are sufficiently close to

one or zero, we further round big ones up to one and truncate small ones to zero. After the rounding-up and truncating, the quantum circuit complexity is reduced while the approximation errors are well-controlled. As a result, the proposed quantum circuit achieves a depth of $O(n)$, for n being the size of the basis set. The extra required number of ancilla qubits is the number of singular values strictly between zero and one.

Using the proposed quantum circuit for the non-unitary linear transformation, we further provide quantum circuit evaluating the inner product of two many-body states under different basis sets in Section IV. Three quantum circuits for the inner product evaluation are proposed with various number of ancilla qubits and measurements. Combining the inner product quantum circuits with the excited state calculation under VQE framework, we could immediately apply different basis optimization for different many-body states, which implement the state-specific CASSCF/OptOrbFCI on quantum computer.

-
- [1] A. Peruzzo, J. McClean, P. Shadbolt, M.-H. Yung, X.-Q. Zhou, P. J. Love, A. Aspuru-Guzik, and J. L. O’Brien, A variational eigenvalue solver on a photonic quantum processor, *Nature Communications* **5**, 4213 (2014).
- [2] B. Bauer, D. Wecker, A. J. Millis, M. B. Hastings, and M. Troyer, Hybrid quantum-classical approach to correlated materials, *Physical Review X* **6**, 031045 (2016), pRX.
- [3] A. Kandala, A. Mezzacapo, K. Temme, M. Takita, M. Brink, J. M. Chow, and J. M. Gambetta, Hardware-efficient variational quantum eigensolver for small molecules and quantum magnets, *Nature* **549**, 242 (2017).
- [4] M. Cerezo, A. Arrasmith, R. Babbush, S. C. Benjamin, S. Endo, K. Fujii, J. R. McClean, K. Mitarai, X. Yuan, and L. Cincio, Variational quantum algorithms, *Nature Reviews Physics* **3**, 625 (2021).
- [5] A. Y. Kitaev, Quantum measurements and the abelian stabilizer problem, arXiv preprint quant-ph/9511026 (1995).
- [6] D. S. Abrams and S. Lloyd, Simulation of many-body fermi systems on a universal quantum computer, *Physical Review Letters* **79**, 2586 (1997), pRL.
- [7] D. S. Abrams and S. Lloyd, Quantum algorithm providing exponential speed increase for finding eigenvalues and eigenvectors, *Physical Review Letters* **83**, 5162 (1998).
- [8] M. A. Nielsen and I. L. Chuang, *Quantum Computation and Quantum Information: 10th Anniversary Edition*, 10th ed. (Cambridge University Press, USA, 2011).
- [9] I. M. Georgescu, S. Ashhab, and F. Nori, Quantum simulation, *Reviews of Modern Physics* **86**, 153 (2014).
- [10] D. Wecker, M. B. Hastings, N. Wiebe, B. K. Clark, C. Nayak, and M. Troyer, Solving strongly correlated electron models on a quantum computer, *Phys. Rev. A* **92**, 062318 (2015).
- [11] I. D. Kivlichan, J. R. McClean, N. Wiebe, C. Gidney, A. Aspuru-Guzik, G. K.-L. Chan, and R. Babbush, Quantum simulation of electronic structure with linear depth and connectivity, *Physical Review Letters* **120**, 110501 (2018).
- [12] R. Babbush, N. Wiebe, J. McClean, J. McClain, H. Neven, and G. K.-L. Chan, Low-depth quantum simulation of materials, *Physical Review X* **8**, 10.1103/physrevx.8.011044 (2018).
- [13] J. C. Slater, Note on hartree’s method, *Physical Review* **35**, 210 (1930).
- [14] J. C. Slater, A simplification of the hartree-fock method, *Physical review* **81**, 385 (1951).
- [15] C. C. J. Roothaan, Self-consistent field theory for open shells of electronic systems, *Reviews of Modern Physics* **32**, 179 (1960), rMP.
- [16] D. Vautherin and D. t. Brink, Hartree-fock calculations with skyrme’s interaction. i. spherical nuclei, *Physical Review C* **5**, 626 (1972).
- [17] E. J. Baerends, D. Ellis, and P. Ros, Self-consistent molecular hartree—fock—slater calculations i. the computational procedure, *Chemical Physics* **2**, 41 (1973).
- [18] E. R. Johnson and A. D. Becke, A post-hartree-fock model of intermolecular interactions, *The Journal of chemical physics* **123** (2005).
- [19] F. Neese, F. Wennmoths, A. Hansen, and U. Becker, Efficient, approximate and parallel hartree—fock and hybrid dft calculations. a ‘chain-of-spheres’ algorithm for the hartree—fock exchange, *Chemical Physics* **356**, 98 (2009).
- [20] P. Siegbahn, A. Heiberg, B. Roos, and B. Levy, A comparison of the super-ci and the newton-raphson scheme in the complete active space scf method, *Physica Scripta* **21**, 323 (1980).
- [21] P. E. Siegbahn, J. Almlöf, A. Heiberg, and B. O. Roos, The complete active space scf (casscf) method in a newton—raphson formulation with application to the hno molecule, *The Journal of Chemical Physics* **74**, 2384 (1981).
- [22] B. O. Roos, P. R. Taylor, and P. E. M. Siegbahn, A complete active space scf method (casscf) using a density matrix formulated super-ci approach, *Chemical Physics*

- 48**, 157 (1980).
- [23] P. J. Knowles and H.-J. Werner, An efficient second-order mc scf method for long configuration expansions, *Chemical Physics Letters* **115**, 259 (1985).
- [24] D. Zgid and M. Nooijen, The density matrix renormalization group self-consistent field method: Orbital optimization with the density matrix renormalization group method in the active space, *The Journal of chemical physics* **128**, 144116 (2008).
- [25] D. Ghosh, J. Hachmann, T. Yanai, and G. Chan, Orbital optimization in the density matrix renormalization group, with applications to polyenes and β -carotene, *The Journal of chemical physics* **128**, 144117 (2008).
- [26] T. Yanai, Y. Kurashige, D. Ghosh, and G. K.-L. Chan, Accelerating convergence in iterative solution for large-scale complete active space self-consistent-field calculations, *International Journal of Quantum Chemistry* **109**, 2178 (2009).
- [27] J. Olsen, The casscf method: A perspective and commentary, *International Journal of Quantum Chemistry* **111**, 3267 (2011).
- [28] S. Wouters, T. Bogaerts, P. Van Der Voort, V. Van Speybroeck, and D. Van Neck, Communication: Dmrgscf study of the singlet, triplet, and quintet states of oxo-mn(salen), *The Journal of Chemical Physics* **140**, 10.1063/1.4885815 (2014).
- [29] L. Freitag, S. Knecht, C. Angeli, and M. Reiher, Multireference perturbation theory with cholesky decomposition for the density matrix renormalization group, *Journal of Chemical Theory and Computation* **13**, 451 (2017), doi: 10.1021/acs.jctc.6b00778.
- [30] J. E. T. Smith, B. Mussard, A. A. Holmes, and S. Sharma, Cheap and near exact casscf with large active spaces, *Journal of Chemical Theory and Computation* **13**, 5468 (2017), doi: 10.1021/acs.jctc.7b00900.
- [31] Q. Sun, J. Yang, and G. K.-L. Chan, A general second order complete active space self-consistent-field solver for large-scale systems, *Chemical Physics Letters* **683**, 291 (2017).
- [32] L. Freitag, Y. Ma, A. Baiardi, S. Knecht, and M. Reiher, Approximate analytical gradients and nonadiabatic couplings for the state-average density matrix renormalization group self-consistent-field method, *Journal of Chemical Theory and Computation* **15**, 6724 (2019), doi: 10.1021/acs.jctc.9b00969.
- [33] D. A. Kreplin, P. J. Knowles, and H.-J. Werner, Second-order mscf optimization revisited. i. improved algorithms for fast and robust second-order casscf convergence, *The Journal of Chemical Physics* **150**, 10.1063/1.5094644 (2019).
- [34] D. S. Levine, D. Hait, N. M. Tubman, S. Lehtola, K. B. Whaley, and M. Head-Gordon, Casscf with extremely large active spaces using the adaptive sampling configuration interaction method, *Journal of Chemical Theory and Computation* **16**, 2340 (2020), doi: 10.1021/acs.jctc.9b01255.
- [35] Y. Li and J. Lu, Optimal orbital selection for full configuration interaction (optorbfcf): Pursuing basis set limit under budget., *Journal of chemical theory and computation* (2020).
- [36] W. Mizukami, K. Mitarai, Y. O. Nakagawa, T. Yamamoto, T. Yan, and Y.-y. Ohnishi, Orbital optimized unitary coupled cluster theory for quantum computer, *Physical Review Research* **2**, 033421 (2020).
- [37] J. Tilly, P. Sriluckshmy, A. Patel, E. Fontana, I. Rungger, E. Grant, R. Anderson, J. Tennyson, and G. H. Booth, Reduced density matrix sampling: Self-consistent embedding and multiscale electronic structure on current generation quantum computers, *Physical Review Research* **3**, 033230 (2021).
- [38] S. Yalouz, B. Senjean, J. Günther, F. Buda, T. E. O'Brien, and L. Visscher, A state-averaged orbital-optimized hybrid quantum-classical algorithm for a democratic description of ground and excited states, *Quantum Science and Technology* **6**, 024004 (2021).
- [39] J. Bierman, Y. Li, and J. Lu, Improving the accuracy of variational quantum eigensolvers with fewer qubits using orbital optimization, *Journal of Chemical Theory and Computation* **19**, 790 (2023), doi: 10.1021/acs.jctc.2c00895.
- [40] J. Bierman, Y. Li, and J. Lu, Qubit count reduction by orthogonally constrained orbital optimization for variational quantum excited-state solvers, *Journal of Chemical Theory and Computation* **20**, 3131 (2024), doi: 10.1021/acs.jctc.3c01297.
- [41] Y. Shen, X. Zhang, S. Zhang, J.-N. Zhang, M.-H. Yung, and K. Kim, Quantum implementation of the unitary coupled cluster for simulating molecular electronic structure, *Physical Review A* **95**, 020501 (2017).
- [42] A. G. Taube and R. J. Bartlett, New perspectives on unitary coupled-cluster theory, *International journal of quantum chemistry* **106**, 3393 (2006).
- [43] J. Lee, W. J. Huggins, M. Head-Gordon, and K. B. Whaley, Generalized unitary coupled cluster wave functions for quantum computation, *Journal of chemical theory and computation* **15**, 311 (2018).
- [44] J. Romero, R. Babbush, J. R. McClean, C. Hempel, P. J. Love, and A. Aspuru-Guzik, Strategies for quantum computing molecular energies using the unitary coupled cluster ansatz, *Quantum Science and Technology* **4**, 014008 (2018).
- [45] A. Anand, P. Schleich, S. Alperin-Lea, P. W. K. Jensen, S. Sim, M. Díaz-Tinoco, J. S. Kottmann, M. Degroote, A. F. Izmaylov, and A. Aspuru-Guzik, A quantum computing view on unitary coupled cluster theory, *Chem. Soc. Rev.* **51**, 1659 (2022).
- [46] H. F. Trotter, On the product of semi-groups of operators, *Proceedings of the American Mathematical Society* **10**, 545 (1959).
- [47] M. Suzuki, Improved trotter-like formula, *Physics Letters A* **180**, 232 (1993).
- [48] N. Hatano and M. Suzuki, Finding exponential product formulas of higher orders, in *Quantum annealing and other optimization methods* (Springer, 2005) pp. 37–68.
- [49] G. Vidal, Efficient classical simulation of slightly entangled quantum computations, *Physical review letters* **91**, 147902 (2003).
- [50] D. Thouless, Stability conditions and nuclear rotations in the hartree-fock theory, *Nuclear Physics* **21**, 225 (1960).
- [51] C.-K. Skylaris, A. A. Mostofi, P. D. Haynes, O. Diéguez, and M. C. Payne, Nonorthogonal generalized wannier function pseudopotential plane-wave method, *Physical Review B* **66**, 035119 (2002).
- [52] C.-K. Skylaris, P. D. Haynes, A. A. Mostofi, and M. C. Payne, Introducing onetep: Linear-scaling density functional simulations on parallel computers, *The Journal of chemical physics* **122** (2005).
- [53] D. Maslov, Linear depth stabilizer and quantum fourier

- transformation circuits with no auxiliary qubits in finite-neighbor quantum architectures, *Phys. Rev. A* **76**, 052310 (2007).
- [54] M. Reck, A. Zeilinger, H. J. Bernstein, and P. Bertani, Experimental realization of any discrete unitary operator, *Phys. Rev. Lett.* **73**, 58 (1994).
- [55] C. A. Jiménez-Hoyos, R. Rodríguez-Guzmán, and G. E. Scuseria, n -electron Slater determinants from nonunitary canonical transformations of fermion operators, *Physical Review A* **86**, 052102 (2012), pRA.
- [56] P.-A. Malmqvist and B. O. Roos, The casscf state interaction method, *Chemical Physics Letters* **155**, 189 (1989).
- [57] J. Pittner, H. Lischka, and M. Barbatti, Optimization of mixed quantum-classical dynamics: Time-derivative coupling terms and selected couplings, *Chemical Physics* **356**, 147 (2009).
- [58] F. Kossoski and P.-F. Loos, State-specific configuration interaction for excited states, *Journal of Chemical Theory and Computation* **19**, 2258 (2023), doi: 10.1021/acs.jctc.3c00057.
- [59] A. Marie and H. G. A. Burton, Excited states, symmetry breaking, and unphysical solutions in state-specific casscf theory, *The Journal of Physical Chemistry A* **127**, 4538 (2023), doi: 10.1021/acs.jpca.3c00603.
- [60] S. Yalouz and V. Robert, Orthogonally constrained orbital optimization: Assessing changes of optimal orbitals for orthogonal multireference states, *Journal of Chemical Theory and Computation* **19**, 1388 (2023), doi: 10.1021/acs.jctc.2c01144.
- [61] S. Saade and H. G. A. Burton, Excited state-specific casscf theory for the torsion of ethylene, *Journal of Chemical Theory and Computation* **20**, 5105 (2024), doi: 10.1021/acs.jctc.4c00212.
- [62] G. Granucci, M. Persico, and A. Toniolo, Direct semiclassical simulation of photochemical processes with semiempirical wave functions, *The Journal of Chemical Physics* **114**, 10608 (2001).
- [63] E. Tapavicza, I. Tavernelli, and U. Rothlisberger, Trajectory surface hopping within linear response time-dependent density-functional theory, *Physical Review Letters* **98**, 023001 (2007), pRL.
- [64] R. Mitrić, U. Werner, and V. Bonacić-Koutecký, Nonadiabatic dynamics and simulation of time resolved photoelectron spectra within time-dependent density functional theory: Ultrafast photoswitching in benzylideneaniline, *The Journal of Chemical Physics* **129**, 10.1063/1.3000012 (2008).
- [65] L. Du and Z. Lan, An on-the-fly surface-hopping program jade for nonadiabatic molecular dynamics of polyatomic systems: Implementation and applications, *Journal of Chemical Theory and Computation* **11**, 1360 (2015), doi: 10.1021/ct501106d.
- [66] F. Plasser, M. Ruckebauer, S. Mai, M. Oettel, P. Marquetand, and L. González, Efficient and flexible computation of many-electron wave function overlaps, *Journal of chemical theory and computation* **12**, 1207 (2016).
- [67] S. Lloyd, Universal quantum simulators, *Science* **273**, 1073 (1996).
- [68] A. Gilyén, Y. Su, G. H. Low, and N. Wiebe, Quantum singular value transformation and beyond: exponential improvements for quantum matrix arithmetics, in *Proceedings of the 51st Annual ACM SIGACT Symposium on Theory of Computing*, STOC 2019 (Association for Computing Machinery, New York, NY, USA, 2019) p. 193–204.
- [69] J. Bierman, Y. Li, and J. Lu, Quantum orbital minimization method for excited states calculation on a quantum computer, *Journal of Chemical Theory and Computation* **18**, 4674 (2022).

Appendix A: Details of Unitary Case

This section gives another proof of Thouless theorem using exterior algebra. The proof offers a more intuitive understanding of the construction process for the non-unitary linear transformations. Additionally, it shows that the wedged map $\wedge \mathbf{u}$ defined in Definition 1 is consistent $U(u; \psi)$ in Thouless theorem and the work Kivlichan *et al.* [11].

Let V be a finite-dimensional Hilbert spaces of dimension n . Operator $\mathbf{u} : V \rightarrow V$ is unitary, and admits (5). Notice that \mathbf{u} is unitary and is a finite dimensional normal operator. The eigendecomposition of \mathbf{u} admits,

$$\mathbf{u} = \sum_{k=1}^n e^{i\phi_k} |\sigma_k\rangle \langle \sigma_k|,$$

for $|\sigma_k\rangle$ being its eigenstate associated with eigenvalue $e^{i\phi_k}$. The eigenstates of \mathbf{u} , $\{|\sigma_k\rangle\}_{k=1}^n$ are orthonormal bases of V . Hence, the set of many-body states, $\{|\sigma_{i_1}\rangle \wedge \cdots \wedge |\sigma_{i_k}\rangle \mid 1 \leq i_1 < \cdots < i_k \leq n, \text{ and } 1 \leq k \leq n\}$ is also a basis of $\wedge V$.

Next, we derive the application of $\wedge \mathbf{u}$ on bases of $\wedge V$. By the definition of $\wedge \mathbf{u}$, we have

$$\wedge \mathbf{u} |\sigma_{i_1}\rangle \wedge \cdots \wedge |\sigma_{i_k}\rangle = e^{\sum_{k=1}^n i\phi_k n_k} |\sigma_{i_1}\rangle \wedge \cdots \wedge |\sigma_{i_k}\rangle, \quad (\text{A1})$$

for all $1 \leq i_1 < \cdots < i_k \leq n$, and $1 \leq k \leq n$, where n_k is defined as,

$$n_k = \begin{cases} 0 & k \notin \{i_1, \dots, i_k\}, \\ 1 & k \in \{i_1, \dots, i_k\}. \end{cases}$$

Notice that n_k plays a similar role as the particle number operator $\mathbf{n}(\sigma_k)$. The right-hand-side of (A1) equals to the application of $\prod_{k=1}^n e^{i\phi_k \mathbf{n}(\nu_k)}$ to $|\sigma_{i_1}\rangle \wedge \cdots \wedge |\sigma_{i_k}\rangle$. Further, we know that all particle number operators commute with each other. Hence, we obtain,

$$\begin{aligned} & \wedge \mathbf{u} |\sigma_{i_1}\rangle \wedge \cdots \wedge |\sigma_{i_k}\rangle \\ &= e^{\sum_{k=1}^n i\phi_k n_k} |\sigma_{i_1}\rangle \wedge \cdots \wedge |\sigma_{i_k}\rangle \\ &= e^{\sum_{k=1}^n i\phi_k \mathbf{n}(\sigma_k)} |\sigma_{i_1}\rangle \wedge \cdots \wedge |\sigma_{i_k}\rangle, \end{aligned}$$

for all $1 \leq i_1 < \cdots < i_k \leq n$, and $1 \leq k \leq n$. We conclude that $\wedge \mathbf{u} = e^{\sum_{k=1}^n i\phi_k \mathbf{n}(\sigma_k)}$.

Comparing to the operator $U(u; \psi)$, the basis in the above derivation is $\{\sigma_k\}_{k=1}^n$, which is different from $\{\psi_k\}_{k=1}^n$ in $U(u; \psi)$. Since both $\{\sigma_k\}_{k=1}^n$ and $\{\psi_k\}_{k=1}^n$ are bases of V , the basis transformation between these

two is unitary. As derived in [35], the transformation of creators and annihilators for two basis sets are

$$\begin{aligned}\mathbf{a}^\dagger(\sigma_k) &= \sum_{m=1}^n \langle \psi_m | \sigma_k \rangle \mathbf{a}^\dagger(\psi_m), \text{ and} \\ \mathbf{a}(\sigma_k) &= \sum_{m=1}^n \langle \sigma_k | \psi_m \rangle \mathbf{a}(\psi_m).\end{aligned}$$

The exponent in $e^{\sum_{k=1}^n \imath \phi_k \mathbf{n}(\sigma_k)} = \wedge \mathbf{u}$ could be rewritten as,

$$\begin{aligned}& \sum_{\ell=1}^n \imath \phi_\ell \mathbf{n}(\sigma_\ell) \\ &= \sum_{\ell=1}^n \imath \phi_\ell \mathbf{a}^\dagger(\sigma_\ell) \mathbf{a}(\sigma_\ell) \\ &= \sum_{\ell=1}^n \imath \phi_\ell \sum_{p=1}^n \langle \psi_p | \sigma_\ell \rangle \mathbf{a}^\dagger(\psi_p) \sum_{q=1}^n \langle \sigma_\ell | \psi_q \rangle \mathbf{a}(\psi_q) \\ &= \sum_{p=1}^n \sum_{q=1}^n \langle \psi_p | \left(\sum_{\ell=1}^n \imath \phi_\ell | \sigma_\ell \rangle \langle \sigma_\ell | \right) | \psi_q \rangle \mathbf{a}^\dagger(\psi_p) \mathbf{a}(\psi_q) \\ &= \sum_{p,q=1}^n \langle \psi_p | (\log \mathbf{u}) | \psi_q \rangle \mathbf{a}^\dagger(\psi_p) \mathbf{a}(\psi_q).\end{aligned}$$

Recall the definition of operator \mathbf{u} under basis $\{\psi_k\}_{k=1}^n$ as in (5). Applying the logarithm matrix function to \mathbf{u} leads to

$$\langle \psi_p | \log \mathbf{u} | \psi_q \rangle = (\log u)_{pq}. \quad (\text{A2})$$

Substituting (A2) into the above exponent expression, we prove the Thouless theorem using exterior algebra,

$$\wedge \mathbf{u} = \exp \left(\sum_{p,q=1}^n (\log u)_{pq} \mathbf{a}^\dagger(\psi_p) \mathbf{a}(\psi_q) \right) = U(\mathbf{u}; \psi).$$

Appendix B: Complex Givens Rotation Operator

This section first derives (12) and (13), and then (19) and (16) in detail.

We first give the derivation of (12). The phase matrix $p_p(\phi)$ multiplies the complex sign $e^{-\imath \phi_p}$ to the p -th row of a matrix. The matrix $p_p(\phi)$ is of form,

$$\text{Diag}\{1, \dots, 1, e^{-\imath \phi_p}, 1, \dots, 1\}.$$

The logarithm of $p_p(\phi)$ is

$$\log p_p(\phi) = -\imath \phi_p E_{pp},$$

where E_{pp} is a zero matrix with a single one at the (p, p) -th position. Substituting the logarithm of $p_p(\phi)$ into

$U(p_p(\phi); \psi)$, we obtain,

$$\begin{aligned}U(p_p(\phi); \psi) &= \exp \left(-\imath \phi_p \sum_{i,j=1}^n (E_{pp})_{ij} \mathbf{a}^\dagger(\psi_i) \mathbf{a}(\psi_j) \right) \\ &= \exp(-\imath \phi_p \mathbf{n}(\psi_p)),\end{aligned}$$

which proves (12).

Then we give the derivation of (13). The Givens rotation matrix $r_{pq}(\theta_{pq})$ eliminating the (p, q) -th entry of a matrix is of form

$$\begin{pmatrix} I_{p-1} & & & \\ & \cos \theta_{pq} & & \sin \theta_{pq} \\ & & I_{q-p-1} & \\ & -\sin \theta_{pq} & & \cos \theta_{pq} \\ & & & & I_{N-q} \end{pmatrix}$$

for $p < q$. Recall the logarithm of a rotation matrix admits,

$$\log \begin{pmatrix} \cos \theta & \sin \theta \\ -\sin \theta & \cos \theta \end{pmatrix} = \begin{pmatrix} 0 & \theta \\ -\theta & 0 \end{pmatrix}.$$

Hence, the logarithm of $r_{pq}(\theta_{pq})$ is

$$\log r_{pq}(\theta_{pq}) = \theta_{pq}(E_{pq} - E_{qp}),$$

where E_{ab} denote a zero matrix with a single one at the (a, b) -th position. Substituting the logarithm of $r_{pq}(\theta_{pq})$ into $U(r_{pq}(\theta_{pq}); \psi)$, we obtain,

$$U(r_{pq}(\theta_{pq}); \psi) \quad (\text{B1})$$

$$= \exp \left(\theta_{pq} \sum_{i,j=1}^n (E_{pq} - E_{qp})_{ij} \mathbf{a}^\dagger(\psi_i) \mathbf{a}(\psi_j) \right) \quad (\text{B2})$$

$$= \exp(\theta_{pq}(\mathbf{a}^\dagger(\psi_p) \mathbf{a}(\psi_q) - \mathbf{a}^\dagger(\psi_q) \mathbf{a}(\psi_p))), \quad (\text{B3})$$

which proves (13).

Now (19) and (16) can be derived based on (12) and (13), respectively.

By matrix function property and (12), the Jordan-Wigner encoded phase rotation admits,

$$\begin{aligned}J_\psi \mathbf{P}_p(\phi; \psi) J_\psi^{-1} &= J_\psi \exp(-\imath \phi \mathbf{n}(\psi_p)) J_\psi^{-1} \\ &= \exp(-\imath \phi J_\psi \mathbf{n}(\psi_p) J_\psi^{-1}).\end{aligned}$$

The Jordan-Wigner encoding of the number operator could be derived from that of creation and annihilation operators as in (14),

$$\begin{aligned}J_\psi \mathbf{n}(\psi_p) J_\psi^{-1} &= J_\psi \mathbf{a}^\dagger(\psi_p) \mathbf{a}(\psi_p) J_\psi^{-1} \\ &= J_\psi \mathbf{a}^\dagger(\psi_p) J_\psi^{-1} J_\psi \mathbf{a}(\psi_p) J_\psi^{-1} \\ &= I_1 \otimes \dots \otimes I_{p-1} \otimes (|1\rangle \langle 0|)(|0\rangle \langle 1|) \otimes I_{p+1} \otimes \dots \otimes I_n \\ &= I_1 \otimes \dots \otimes I_{p-1} \otimes \begin{pmatrix} 0 & 0 \\ 0 & 1 \end{pmatrix} \otimes I_{p+1} \otimes \dots \otimes I_n\end{aligned}$$

Hence, we have,

$$\begin{aligned}
& J_\psi \mathbf{P}_p(\phi; \psi) J_\psi^{-1} \\
&= \exp \left(I_1 \otimes \cdots \otimes I_{p-1} \otimes \begin{pmatrix} 0 & 0 \\ 0 & -i\phi \end{pmatrix} \otimes I_{p+1} \otimes \cdots \otimes I_n \right) \\
&= I_1 \otimes \cdots \otimes I_{p-1} \otimes \begin{pmatrix} 1 & 0 \\ 0 & e^{-i\phi} \end{pmatrix} \otimes I_{p+1} \otimes \cdots \otimes I_n.
\end{aligned}$$

Similarly, by matrix function property and (13), we could derive the Jordan-Wigner encoded Givens rotation. For simplicity, we give the derivation for $p = q - 1$ in detail, which is the only Givens rotation used in [11]. We omit the subscript in $\theta_{pq} = \theta_{q-1,q}$ in the following, and the Jordan-Wigner encoded Givens rotation admits,

$$\begin{aligned}
& J_\psi \mathbf{R}_{q-1,q}(\theta; \psi) J_\psi^{-1} \\
&= \exp \left(J_\psi (\theta (\mathbf{a}^\dagger(\psi_{q-1}) \mathbf{a}(\psi_q) - \mathbf{a}^\dagger(\psi_q) \mathbf{a}(\psi_{q-1}))) J_\psi^{-1} \right) \\
&= \exp \left(I_1 \otimes \cdots \otimes I_{q-2} \otimes \begin{pmatrix} 0 & 0 & 0 & 0 \\ 0 & 0 & \theta & 0 \\ 0 & -\theta & 0 & 0 \\ 0 & 0 & 0 & 0 \end{pmatrix} \otimes \cdots \otimes I_n \right) \\
&= I_1 \otimes \cdots \otimes I_{q-2} \otimes \begin{pmatrix} 1 & 0 & 0 & 0 \\ 0 & \cos \theta & \sin \theta & 0 \\ 0 & -\sin \theta & \cos \theta & 0 \\ 0 & 0 & 0 & 1 \end{pmatrix} \otimes \cdots \otimes I_n.
\end{aligned}$$